1	
2	
3	
4	
5	
6	
7	
8	
9	
10	
11	Nutrient and arsenic biogeochemistry of Sargassum in the western Atlantic
12	
13	D.J. McGillicuddy, Jr. <sup>1</sup>
14	P.L. Morton <sup>2</sup>
15	R.A. Brewton <sup>3</sup>
16	C. Hu <sup>4</sup>
17	T.B. Kelly <sup>5</sup>
18	A.R. Solow <sup>1</sup>
19	B.E. Lapointe <sup>3</sup>
20	- -
21	Manuscript revised and resubmitted to Nature Communications
22	
23	August 17, 2023
24	
25	
26	
27	
28	
29	
30	
31	
32	<sup>1</sup> Department of Applied Ocean Physics and Engineering, Woods Hole Oceanographic Institution,
33	Woods Hole, MA 02543, USA. Tel: 508-289-2683 Fax: 508-457-2194 Email:
34	dmcgillicuddy@whoi.edu (Corresponding Author).
35	<sup>2</sup> Department of Oceanography, Texas A&M University, College Station, TX, USA.
36	<sup>3</sup> Harbor Branch Oceanographic Institute, Florida Atlantic University, Fort Pierce, FL, USA.
37	<sup>4</sup> College of Marine Science, University of South Florida, St. Petersburg, FL, USA.
38	<sup>5</sup> College of Fisheries and Ocean Science, University of Alaska Fairbanks, Fairbanks, AK, USA.
39	

The oceanographic ecology of pelagic Sargassum, and the means by which these floating macroalgae thrive in the nutrient-poor waters of the open ocean, have been studied for decades. Beginning in 2011, the Great Atlantic Sargassum Belt (GASB) emerged, with Sargassum proliferating in the tropical Atlantic and Caribbean where it had not previously been abundant. Here we show that the nutritional status of Sargassum in the GASB is distinct, with higher nitrogen and phosphorus content than populations residing in its Sargasso Sea habitat. Moreover, we find that variations in arsenic content of Sargassum reflect phosphorus limitation, following a hyperbolic relationship predicted from Michaelis-Menten nutrient uptake kinetics. Although the sources of nutrients fueling the GASB are not yet clear, our results suggest that nitrogen and phosphorus content of Sargassum, together with its isotopic composition, can be used to identify those sources, whether they be atmospheric, oceanic, or riverine in origin.

The floating macroalgae *Sargassum* spp. serves as a habitat for more than 200 types of organisms, including 10 endemic species<sup>1-3</sup> and provides habitat for fish nursery, spawning and foraging<sup>4,5</sup>. Neonate and juvenile sea turtles use *Sargassum* habitat for feeding as well as protection from predators<sup>6,7</sup>, and several species of seabirds forage over *Sargassum*<sup>8,9</sup>. In contrast to these traditionally beneficial ecological impacts, the GASB's unprecedented inundations of *Sargassum* on Caribbean and Florida coastlines have had deleterious effects on near-shore seagrass and coral reef ecosystems<sup>10-13</sup>, and have led to declines in turtle hatchling survival<sup>14</sup>. The GASB has also presented challenges to regional economies, particularly those that rely heavily on tourism<sup>15,16</sup>. *Sargassum* decay on coastal margins can cause respiratory and other human health issues<sup>17</sup>, and the presence of arsenic in *Sargassum* tissue<sup>18-20</sup> puts significant constraints on utilization of the biomass that washes ashore<sup>21-23</sup>.

A complex set of interconnected hypotheses have been offered to explain dynamics of the GASB<sup>24-26</sup>. Anomalous wind patterns in 2009-2010 are thought to have introduced *Sargassum* from its habitat in the Sargasso Sea into the eastern North Atlantic where it was subsequently entrained into the equatorial current system<sup>27</sup>. Since that time, *Sargassum* has increased dramatically in the tropical Atlantic, begging the question of nutrient supply. A variety of nutrient sources have been suggested<sup>26-29</sup>, including upwelling, vertical mixing, discharge from the Amazon and Congo rivers, and atmospheric deposition. However, the causes of the GASB and the mechanisms controlling its seasonal to interannual variability remain unknown. An underlying question is: is this massive abundance of *Sargassum* a result of higher nutrient availability in the GASB?

In this work we show that GASB *Sargassum* populations are enriched in both nitrogen and phosphorus content relative to its Sargasso Sea habitat, clearly identifying nutrient supply as a primary driver of this phenomenon. In addition, we demonstrate that *Sargassum*'s arsenic content varies with the degree of phosphorus limitation, linking our observations with a theoretical prediction based on nutrient uptake kinetics. Our results show that ascertaining the nutrient sources and their regulation is essential to understand the underlying causes of this basin-scale phenomenon—and only then will society have a conceptual basis on which to design potential strategies to mitigate the consequences of the GASB.

### Results

### Sargassum distributions and nutritional status

In order to address this question, *Sargassum* tissue samples were collected in spring 2021 along with hydrographic and nutrient measurements on two hydrographic sections in the western

Atlantic (Methods) that intersected the western portion of the GASB (Fig. 1). The samples were separated into two species *S. fluitans* and *S. natans* based on their morphology<sup>30</sup>. *S. fluitans* and *S. natans* co-occurred in the southern portions of both A20 and A22. *S. natans* was more prevalent north of 24°N on A22, and north of 27°N on A20. Both species were present at 32°N on A20 as well as the farthest north sample, collected just south of the Gulf Stream on A22.

Sargassum elemental composition was similar between species (Fig. 2, Supplementary Table 1), a finding that is consistent with earlier studies<sup>29</sup>. Our data reveal three distinct regimes within the sampling domain. In the Sargasso Sea, carbon content tends to be relatively high (particularly in the eastern transect A20), whereas nitrogen and phosphorus content tend to be low. Nutritional status in the GASB was much better, with nitrogen and phosphorus content of Sargassum in the Caribbean and western tropical Atlantic significantly higher than in the Sargasso Sea (Supplementary Fig. 1, Supplementary Table 2). Interestingly, nitrogen and phosphorus content were highest in the northern Sargasso Sea.

These trends are also evident in elemental ratios (Supplementary Fig. 2). As expected, C:N was high in the Sargasso Sea, driven by higher carbon content and lower nitrogen content (Fig. 2). These ratios are higher in A20 than in A22, particularly in *S. natans*. This zonal gradient with C:N increasing to the east is driven by both increasing carbon content and decreasing nitrogen content. C:P is also high in the Sargasso Sea, although the zonal gradient evident in C:N is not clear in C:P. N:P shows a pronounced maximum in the Sargasso Sea region of A22, which is driven by a combination of increased N content and decreased P content. Little meridional trend in N:P is evident in A20, and in aggregate N:P in the Sargasso Sea differs less from the surrounding regions than does C:N and C:P (Supplementary Fig. 1).

Based on the seasonal analysis conducted on prior data sets<sup>29</sup>, the springtime samples described herein would be expected to be at their seasonal maxima of nitrogen and phosphorus content, and minima of their C:N and C:P ratios.

### **Nutrient sources**

Because *Sargassum* is subject to both surface currents and wind, hydrodynamic transport plays a key role in its dynamics<sup>31-33</sup>. In order to assess the recent history of our *Sargassum* samples, passive particles were inserted into a numerical ocean model hindcast at each collection site and tracked backward in time (Fig. 3; see Methods). The southernmost sample of A20 appears to have come from the southeast, whereas samples in the 10-30°N latitude band come primarily from the east. Exceptions to that pattern include an eddy-like flows from 25°N to 28°N on A22. Samples collected north of 30°N on A20 appear to have come from the north, consistent with a Gulf Stream origin. The northernmost sample on A22 was clearly under the influence of the Gulf Stream, although its point of entry into the Gulf Stream varied widely within the ensemble—ranging from the continental shelf north of Cape Hatteras to the South Atlantic Bight, with some in the core of the Gulf Stream as far south as 30°N.

This information, together with  $\delta^{15}N$  values of the *Sargassum* tissue, facilitates some inferences about nitrogen sources. Specifically, *Sargassum* utilizing riverine nitrogen tend to have enriched (positive)  $\delta^{15}N$  values, whereas those fueled by near-surface oceanic and atmospheric sources have lower (negative to slightly positive)  $\delta^{15}N$  values<sup>29</sup>. Nitrogen fixation typically results in a fractionation of -2‰<sup>34</sup>.

Patterns in  $\delta^{15}$ N from our survey reveal spatial coherence, with no systematic difference between *S. fluitans* and *S. natans* (Fig. 2). Depleted  $\delta^{15}$ N values in the Sargasso Sea, Caribbean, and western tropical Atlantic could result from nitrogen fixation by epiphytic cyanobacteria<sup>35,36</sup>

or perhaps atmospheric deposition<sup>37</sup>. The highest  $\delta^{15}$ N values occurred in the northern Sargasso Sea, with values of approximately +2% potentially reflecting riverine sources along the U.S. east coast (as indicated by spatial connectivity depicted in Fig. 3), or as distant as the Gulf of Mexico which has been identified as a source region for *Sargassum* in the western Atlantic<sup>38</sup>. For example, a coherent plume emanating from the Mississippi River in summer of 2004 was entrained into the Loop Current, reaching the Straits of Florida in approximately 25 days, continuing northward in the Gulf Stream to be found in the South Atlantic Bight another 25 days after that<sup>39</sup>. Our northern Sargasso Sea samples were collected another 600 nm farther downstream, so assuming a flow of 4 kt, they could have been influenced by Mississippi River water discharged as recently as 150 days before sampling. With end-member  $\delta^{15}$ N values of +6-8‰ in in northern Gulf of Mexico Sargassum<sup>29</sup>, dilution to +2‰ would require several doublings of the population using oceanic sources of nitrogen—which is certainly possible based on observed growth rates<sup>36,40,41</sup>. Alternatively, enrichment of  $\delta^{15}N$  in samples from the northern Sargasso Sea could be caused by upwelling and/or vertical mixing, as values of +2% are characteristic of nitrate in the upper thermocline in that region<sup>42,43</sup>. 

Enriched  $\delta^{15}N$  values were also found in the southernmost samples of the western tropical Atlantic (Fig. 2), under direct influence of the Amazon River plume (as evidenced by the salinity distribution in Fig. 1) which has been implicated as a nutrient source for the GASB<sup>26-29,44</sup>. There was one station in the Caribbean interior (17°N, 67°W) where similarly high  $\delta^{15}N$  values were measured, but the corresponding salinity (Fig. 1) does not be speak riverine influence. Particle backtracking calculations suggest source waters to the east-southeast (Fig. 3), and given the cross-isohaline transport enabled by wind drag, Amazon River influence is plausible. However, it is noteworthy that neither the elemental composition (Fig. 2) nor nutrient ratios (Supplementary Fig. 2) in the high- $\delta^{15}N$  samples of the tropical Atlantic and Caribbean Sea show corresponding anomalies.

Hydrographic data from sections A20 and A22 provide environmental information with which to interpret the *Sargassum* observations. The nitracline and phosphocline are deepest in the warm and salty waters of the Sargasso Sea, and shallower in the warmer and fresher waters of the Caribbean and western tropical Atlantic (Supplementary Fig. 3). Both nutriclines are shallower in the colder and fresher waters of the northern Sargasso Sea. Near-surface nutrient concentrations are generally very low except for the northernmost portions of each transect where the nutriclines outcrop. Nitrate and phosphate are at or below the limit of detection in the surface waters Sargasso Sea (Supplementary Fig. 4). Nitrate is enhanced in the Caribbean, and less so in the western tropical Atlantic, where surface phosphate is elevated. The presence of detectable nitrate and phosphate in these areas is consistent with the enhanced nutritional status of *Sargassum* in the GASB.

### **Arsenic biogeochemistry**

The fact that *Sargassum* bioaccumulates arsenic has generated considerable interest, particularly because the associated toxicity puts practical limitations on valorization of the biomass inundating coastal communities of the GASB. Our survey revealed regional scale variations in arsenic content (Fig. 2). Arsenic content was lowest in the GASB (Caribbean and Western Tropical Atlantic samples) and highest in the Sargasso Sea, particularly in the eastern transect A20. Other stations in A20 show modest enrichment, such as in the southernmost samples at 9°N, 52°W and the Northern Sargasso Sea samples at 31-33°N, 52°W. There are no

systematic differences in arsenic content between *S. fluitans* and *S. natans* (Supplementary Table 1), although interspecies variability is apparent at some stations (Fig. 2).

The high arsenic content of *Sargassum* in the subtropical gyre is accompanied by the lowest phosphorus content, which is consistent with the depression of the phosphocline (Supplementary Fig. 3) and surface dissolved phosphate concentrations generally below the limit of detection (Supplementary Fig. 4). Thus, the arsenic to phosphorus ratio of *Sargassum* of the subtropical gyre stands out as uniquely high in that region (Fig. 2), where *Sargassum* is known to be phosphorus limited<sup>45</sup>.

Uptake of arsenate (AsO<sub>4</sub><sup>3-</sup>) by aquatic plants occurs as a byproduct of phosphorus uptake, owing to its chemical similarity with the phosphate ion (PO<sub>4</sub><sup>3-</sup>)<sup>46,47</sup>. Using the standard Michaelis-Menten form, uptake of dissolved phosphate and arsenate can be expressed as:

$$\rho_P = \mu_P \frac{[PO_4^{3-}]}{k_P + [PO_4^{3-}]}$$
 and  $\rho_{AS} = \mu_{AS} \frac{[AsO_4^{3-}]}{k_{AS} + [AsO_4^{3-}]}$ 

For low concentrations of phosphate and arsenate, uptake is approximately linear in concentration:

$$ho_P pprox \mu_P rac{[ ext{PO}_4^{3^-}]}{k_P} \qquad ext{and} \qquad 
ho_{AS} pprox \mu_{AS} rac{[ ext{AsO}_4^{3^-}]}{k_{AS}}$$

The ratio of As to P uptake is therefore:

196 
$$\frac{\rho_{As}}{\rho_{P}} = \frac{\mu_{As} k_{p}}{\mu_{P} k_{As}} \frac{[\text{AsO}_{4}^{3-}]}{[\text{PO}_{4}^{3-}]}$$

Surface arsenate concentrations in the tropical and subtropical Atlantic are relatively uniform in comparison with phosphate, and up to an order of magnitude lower<sup>48</sup>. Moreover, surface concentrations of arsenate and phosphate are uncorrelated<sup>49</sup>, so the ratio of As to P uptake can be simplified to:

$$\frac{\rho_{As}}{\rho_P} \sim \frac{1}{[PO_4^{3-}]}$$
204

Assuming that the tissue content of these two constituents reflects their proportionate uptake, one would expect that the ratio of arsenic to phosphorus in *Sargassum* would be a hyperbolic function of phosphorus content:

$$\frac{\% As}{\% P} \sim \frac{1}{\% P}$$

This prediction is qualitatively consistent with the present data as well as prior observations dating back to the 1980s (Fig. 4), although the dependence on phosphorus content varies as %P<sup>-1.3</sup> rather than %P<sup>-1.0</sup> predicted by the theory. The reason for this supra-hyperbolic dependence is not known, but it is statistically reliable with a p-value <0.001 (Supplementary Note). This is a clear demonstration of arsenic content as a diagnostic of phosphorus limitation in a natural population of marine algae, and is consistent with laboratory studies<sup>50,51</sup>, biogeochemical proxies based on dissolved As speciation in the ocean<sup>49</sup>, and other recent field data<sup>52</sup>.

It could be argued that the As:P versus P relationship in Fig. 4 is a result of the intrinsic association among variables: for two random variables a and b, plotting the ratio a:b versus b will take on a hyperbolic form. However, the elemental composition of *Sargassum* is not random. For example, the As:C ratio does not show a hyperbolic dependence on carbon content (Supplementary Fig. 5). Interestingly, As:N varies hyperbolically with nitrogen content, which we attribute to covariation in nitrogen and phosphorus content.

Notwithstanding our theoretical prediction of the hyperbolic relationship of As:P and P content, one might also expect a negative correlation between As and P content as a symptom of phosphorus stress in *Sargassum*. Observations are also consistent with this expectation (Supplementary Fig. 6). A similar negative correlation is observed between arsenic and nitrogen content, which we again attribute to the correlation between nitrogen and phosphorus content. In contrast, As content is positively correlated with carbon content.

#### **Discussion**

Nutrient limitation of oceanic *Sargassum* populations in their native habitat was demonstrated decades ago<sup>45,53</sup>, and enhanced nutrient availability has been advanced as a key factor in stimulating the GASB<sup>26,27,29</sup>. We show clearly for the first time that *Sargassum* in the GASB is enhanced in both nitrogen and phosphorus, indicative of a healthy and thriving population. Stable nitrogen isotope values point to riverine sources in some circumstances, and are more equivocal in others. Distinguishing the various nutrient sources sustaining the GASB will require systematic snapshots of nutrient content and isotopic composition across its entire breadth. Presumably, the closer one gets to the source, the higher the nitrogen and / or phosphorus content of *Sargassum* should be. In that sense, basin-wide patterns in nitrogen and phosphorus elemental composition could provide the fingerprinting necessary to unequivocally determine the sources. However, given the strong seasonal to interannual variability intrinsic to the GASB, it will be essential that such snapshots be synoptic, which poses significant practical challenges for a phenomenon of this scale.

Our novel demonstration of arsenic content as an indicator of phosphorus stress in natural populations of *Sargassum* also has considerable implications. *Sargassum* inundating coastal areas of the GASB already contains arsenic concentrations that can exceed safe thresholds for consumption<sup>21-23</sup>. If the phosphorus supply to the GASB were to wane relative to that of nitrogen, our findings would suggest that arsenic content of *Sargassum* in that area would rise even further, perhaps up to levels currently observed in the Sargasso Sea. This would have important implications for management if the nutrient sources turn out to be anthropogenic.

For all these reasons, expanded observational and modeling studies are needed to understand the GASB's physical, biological, and chemical drivers. Moreover, the societal need for scientific understanding is urgent: improved seasonal to interannual predictions would offer tremendous value for proactive planning and response, while quantification of the underlying causes could inform potential management actions to mitigate the problem.

#### Methods

Sampling was conducted on R/V *Thomas G. Thompson* voyages TN389 (16 March – 16 April 2021) and TN390 (20 April – 16 May 2021), occupying GO-SHIP lines A20<sup>54</sup> and A22<sup>55</sup>, respectively.

*Hydrography* 

Hydrographic profiles and water samples were collected with a standard Conductivity, Temperature, Depth (CTD) rosette system with Niskin bottles. Nutrient analyses were carried out at sea using a Seal Analytical continuous-flow AutoAnalyzer 3, consistent with the methods described in the GO-SHIP repeat hydrography manual<sup>56</sup>.

## Sargassum collection and identification

Sargassum spp. samples were collected with a dip net and sorted into the species and morphotypes, S. natans I and S. fluitans III per Parr <sup>30</sup>. Recent literature has indicated the increasing presence of a previously rare form S. natans V III on the basis of both morphology<sup>25</sup> and genetics<sup>57,58</sup>. Based on morphological similarity, any S. natans V III in our samples would have been classified as S. fluitans III.

## Sargassum elemental analysis and isotopic composition

Samples for each morphotype were separated into up to three replicates as quantities allowed (6 to 10 thalli/species), rinsed briefly (3 to 5 s) in deionized water, cleaned of macroscopic epizoa and epiphytes, dried in a laboratory oven at 65 to 70°C for 48 h, and powdered with a mortar and pestle <sup>53</sup>. The dried *Sargassum* samples were split in half and stored in plastic screw top vials. One half was used for arsenic analysis (see below), and the other half was shipped to the University of Georgia's Center for Applied Isotope Studies Stable Isotope Ecology Laboratory (UGA-SIEL; https://cais.uga.edu/facilities/stable-isotope-ecology-laboratory/) for analysis of  $\delta^{15}$ N as well as %C and %N on a Thermo Delta V IRMS coupled to a Carlo Erba NA1500 CHN-Combustion Analyzer via a Thermo Conflo Interface. National Institute of Standards and Technology reference materials 8549, 8558, 8568, and 8569 were used to routinely calibrate working standards prepared in the laboratory. QA/QC results were incorporated into the raw data reports received by UGA-SIEL. The other part of this half sample was analyzed at UGA-SIEL for %P, where approximately 2 mg of dried tissue was weighed into crucibles, ashed at 500 °C for four hours and extracted with 0.2 mL of Aqua Regia acid<sup>59,60</sup>. The acid extracts were then diluted 41:1 with deionized water for TP (as PO<sub>4</sub>-P) analysis on an Alpkem 300 series analyzer.

### Sargassum arsenic content

Arsenic content of *Sargassum* tissue was measured by the University of Missouri Soil and Plant Testing Laboratory (MU SPTL) using an Inductively Coupled Plasma Optical Emission Spectrometer (ICP-OES; Agilent 5800; λ<sub>As</sub> = 188.980 nm). Subsamples of rinsed, dried, and powdered *Sargassum* tissue from the GO-SHIP A20/A22 expeditions were digested at MU SPTL in 2022 according to EPA method 3052. In brief, the powdered samples were digested with a combination of HNO<sub>3</sub> acid at 175°C for 15 minutes using a microwave-accelerated digestion system (CEM MARS Xpress). Samples collected prior to the 2021 surveys were retrieved from the B. Lapointe archives (1980-2018) at the Harbor Branch Oceanographic Institute, Florida Atlantic University. Prior to sending to the MU SPTL for ICP-OES analysis, this subset was digested at the National High Magnetic Field Laboratory at Florida State University (P. Morton) in 2020 following a two-step process. First, ~0.1 g aliquots of powdered sample were carefully weighed into 15-mL Teflon digestion beakers (Savillex), to which 3 mL of concentrated HNO<sub>3</sub> acid (Fisher Optima) were added. The beakers were tightly capped and left overnight (~12 hours) on a hotplate at 150°C. The beakers were then uncapped, and the digested sample taken to dryness (150°C, 2-4 hrs). The sample residue was then digested a second time (capped, 150°C,

overnight) using 3 mL concentrated HNO<sub>3</sub> (Fisher Optima) and 200 μL of concentrated HF (Fisher Optima). The samples were taken to dryness again (uncapped, 150°C) and the residue dissolved in 3.0 mL of 0.32 M HNO<sub>3</sub> (Fisher Optima).

All samples were analyzed at MU SPTL with ICAP-OES at a 1/100 dilution to bring the As concentrations into working range of the matrix-matched (0.16 M HNO<sub>3</sub>) external standard calibration curve. Triplicate independent digestions and analyses of four *Sargassum* tissue samples were used to determine the representative reproducibility of the sample processing and instrumental analysis methods. For more details see

https://extension.missouri.edu/programs/soil-and-plant-testing-laboratory/spl-researchers.

## Backtracking of source waters

At each station where *Sargassum* was collected, the source waters were assessed by tracking particles backward in time for 60 days using a Lagrangian algorithm<sup>61</sup>. Surface currents were specified from the OSCAR 1/3° resolution analysis, described at <a href="https://www.esr.org/research/oscar/oscar-surface-currents/">https://www.esr.org/research/oscar/oscar-surface-currents/</a> and available at <a href="https://podaac.jpl.nasa.gov/dataset/OSCAR\_L4\_OC\_third-deg">https://podaac.jpl.nasa.gov/dataset/OSCAR\_L4\_OC\_third-deg</a>. A total of 100 particles were released at each location where *Sargassum* was found, with random walk diffusion applied each time step  $\Delta t$  with gaussian perturbations  $\sigma$  defined by  $\sigma^2 = 4D\Delta t$ . The horizontal diffusivity D was chosen to be 4000 m² s¹ based on estimates for this region derived from Argo float observations<sup>62</sup>. In addition to being affected by surface currents, wind also influences

330 Sargassum transport<sup>31,32</sup>. Windage factors ranging from 0.5% and 3% produce the most accurate simulations of Sargassum trajectories<sup>63,64</sup>, and a mid-point value of 2% was used here. Wind

forcing was specified using daily NCEP/NCAR reanalysis<sup>65</sup> and validated with shipboard

meteorological measurements made on R/V *Thomas G. Thompson* during voyages TN389 and TN390.

### Satellite observations

Pelagic *Sargassum* distributions were derived from MODIS measurements using a floating algal index<sup>26,66,67</sup>. MODIS data were obtained from the U.S. National Aeronautics and Space Administration (NASA) Goddard Space Flight Center (https://oceancolor.gsfc.nasa.gov). Surface salinity distributions were obtained from SMOS Earth Explorer mission and the data were accessed on <a href="https://www.catds.fr/Products/Available-products-from-CPDC">https://www.catds.fr/Products/Available-products-from-CPDC</a>.

### Data availability

Sargassum tissue data are available as separate files in the Supplementary Information.

### Shipboard hydrographic data:

https://cchdo.ucsd.edu/cruise/325020210316 (TN389) https://cchdo.ucsd.edu/cruise/325020210420 (TN390)

### Surface currents used for particle tracking:

https://podaac.jpl.nasa.gov/dataset/OSCAR\_L4\_OC\_third-deg

### Satellite-based surface salinity:

https://www.catds.fr/Products/Available-products-from-CPDC

356 357	Raw d	ata for computation of satellite-based <i>Sargassum</i> distributions: <a href="https://oceancolor.gsfc.nasa.gov">https://oceancolor.gsfc.nasa.gov</a>
358 359 360	Sargas	ssum density distribution maps: <a href="https://optics.marine.usf.edu/projects/saws.html">https://optics.marine.usf.edu/projects/saws.html</a>
361 362 363 364		availability e tracking code: <a href="https://doi.org/10.5281/zenodo.3468524">https://doi.org/10.5281/zenodo.3468524</a>
365	Refere	ences
366 367 368 369	1	Martin, L. M. <i>et al.</i> Pelagic <i>Sargassum</i> morphotypes support different rafting motile epifauna communities. <i>Marine Biology</i> <b>168</b> , 115 (2021). <a href="https://doi.org:10.1007/s00227-021-03910-2">https://doi.org:10.1007/s00227-021-03910-2</a>
370 371 372	2	Coston-Clements, L., Settle, L. R., Hoss, D. E. & Cross, F. A. Utilization of the <i>Sargassum</i> habitat by marine invertebrates and vertebrates, a review. <i>NOAA technical memorandum NMFS-SEFSC 296</i> (1991).
373 374 375	3	Huffard, C. L., von Thun, S., Sherman, A. D., Sealey, K. & Smith, K. L. Pelagic <i>Sargassum</i> community change over a 40-year period: temporal and spatial variability. <i>Marine Biology</i> <b>161</b> , 2735-2751 (2014). <a href="https://doi.org/10.1007/s00227-014-2539-y">https://doi.org/10.1007/s00227-014-2539-y</a>
376 377 378	4	NMFS. National Marine Fisheries Service: Fisheries of the Caribbean, Gulf of Mexico and South Atlantic; pelagic <i>Sargassum</i> habitat of the south Atlantic region (Final Rule). <i>Federal Register</i> <b>68</b> , 57375 (2003).
379 380 381	5	ICCAT. Resolution 05–11 on pelagic Sargassum. Compendium Management Recommendations and Resolutions adopted by ICCAT for the Conservation of Atlantic tunas and tuna-like species (2005).
382 383 384	6	Mansfield, K. L., Wyneken, J., Porter, W. P. & Luo, J. First satellite tracks of neonate sea turtles redefine the 'lost years' oceanic niche. <i>Proc Biol Sci</i> <b>281</b> , 20133039 (2014). <a href="https://doi.org:10.1098/rspb.2013.3039">https://doi.org:10.1098/rspb.2013.3039</a>
385 386 387	7	Witherington, B., Hirama, S. & Hardy, R. Young sea turtles of the pelagic <i>Sargassum</i> -dominated drift community: habitat use, population density, and threats. <i>Marine Ecology Progress Series</i> <b>463</b> , 1-22 (2012).
388 389	8	Haney, J. C. Seabird Patchiness in Tropical Oceanic Waters: The Influence of <i>Sargassum</i> "Reefs". <i>The Auk</i> <b>103</b> , 141-151 (1986). <a href="https://doi.org:10.1093/auk/103.1.141">https://doi.org:10.1093/auk/103.1.141</a>
390 391	9	Moser, M. L. & Lee, D. S. Foraging over <i>Sargassum</i> by western North Atlantic seabirds. <i>The Wilson Journal of Ornithology</i> <b>124</b> , 66-72 (2012).
392 393 394	10	van Tussenbroek, B. I. <i>et al.</i> Severe impacts of brown tides caused by <i>Sargassum</i> spp. on near-shore Caribbean seagrass communities. <i>Marine Pollution Bulletin</i> <b>122</b> , 272-281 (2017). <a href="https://doi.org/10.1016/j.marpolbul.2017.06.057">https://doi.org/10.1016/j.marpolbul.2017.06.057</a>

395 396 397	11	Rodríguez-Martínez, R. E. <i>et al.</i> Faunal mortality associated with massive beaching and decomposition of pelagic <i>Sargassum</i> . <i>Marine Pollution Bulletin</i> <b>146</b> , 201-205 (2019). <a href="https://doi.org/10.1016/j.marpolbul.2019.06.015">https://doi.org/10.1016/j.marpolbul.2019.06.015</a>
398 399 400	12	Alvarez-Filip, L., Estrada-Saldívar, N., Pérez-Cervantes, E., Molina-Hernández, A. & González-Barrios, F. J. A rapid spread of the stony coral tissue loss disease outbreak in the Mexican Caribbean. <i>PeerJ</i> 7, e8069 (2019). <a href="https://doi.org.10.7717/peerj.8069">https://doi.org.10.7717/peerj.8069</a>
401 402 403 404	13	Cabanillas-Terán, N., Hernández-Arana, H., Ruiz-Zárate, M., Vega-Zepeda, A. & Sanchez-Gonzalez, A. <i>Sargassum</i> blooms in the Caribbean alter the trophic structure of the sea urchin <i>Diadema antillarum</i> . <i>PeerJ</i> 7:e7589 <a href="https://doi.org/10.7717/peerj.7589">https://doi.org/10.7717/peerj.7589</a> (2019).
405 406 407	14	Maurer, A. S., De Neef, E. & Stapleton, S. <i>Sargassum</i> accumulation may spell trouble for nesting sea turtles. <i>Frontiers in Ecology and the Environment</i> <b>13</b> , 394-395 (2015). <a href="https://doi.org/10.1890/1540-9295-13.7.394">https://doi.org/10.1890/1540-9295-13.7.394</a>
408 409	15	Louime, C., Fortune, J. & Gervais, G. <i>Sargassum</i> invasion of coastal environments: a growing concern. <i>American Journal of Environmental Sciences</i> <b>13.1</b> , 58-64 (2017).
410 411 412 413 414	16	United Nations Environment Programme. <i>Sargassum</i> White Paper - <i>Sargassum</i> Outbreak in the Caribbean: Challenges, Opportunities and Regional Situation. <i>Eighth Meeting of the Scientific and Technical Advisory Committee (STAC) to the Protocol Concerning Specially Protected Areas and Wildlife (SPAW) in the Wider Caribbean Region, <a href="https://wedocs.unep.org/20.500.11822/35948">https://wedocs.unep.org/20.500.11822/35948</a>. (2018).</i>
415 416 417	17	Resiere, D. <i>et al. Sargassum</i> seaweed on Caribbean islands: an international public health concern. <i>Lancet (London, England)</i> <b>392</b> , 2691 (2018). <a href="https://doi.org:10.1016/s0140-6736(18)32777-6">https://doi.org:10.1016/s0140-6736(18)32777-6</a>
418 419 420 421	18	Dassié, E. P., Gourves, PY., Cipolloni, O., Pascal, PY. & Baudrimont, M. First assessment of Atlantic open ocean <i>Sargassum</i> spp. metal and metalloid concentrations. <i>Environmental Science and Pollution Research</i> <b>29</b> , 17606-17616 (2022). <a href="https://doi.org:10.1007/s11356-021-17047-8">https://doi.org:10.1007/s11356-021-17047-8</a>
422 423 424	19	Johnson, D. L. & Braman, R. S. The speciation of arsenic and the content of germanium and mercury in members of the pelagic <i>Sargassum</i> community. <i>Deep Sea Research</i> 22, 503-507 (1975). <a href="https://doi.org/10.1016/0011-7471(75)90023-6">https://doi.org/10.1016/0011-7471(75)90023-6</a>
425 426 427	20	Cipolloni, OA. <i>et al.</i> Metals and metalloids concentrations in three genotypes of pelagic <i>Sargassum</i> from the Atlantic Ocean Basin-scale. <i>Marine Pollution Bulletin</i> <b>178</b> , 113564 (2022). <a href="https://doi.org/10.1016/j.marpolbul.2022.113564">https://doi.org/10.1016/j.marpolbul.2022.113564</a>
428 429 430	21	Rodríguez-Martínez, R. E. <i>et al.</i> Element concentrations in pelagic <i>Sargassum</i> along the Mexican Caribbean coast in 2018-2019. <i>PeerJ</i> <b>8</b> (2020). <a href="https://doi.org/10.7717/peerj.8667">https://doi.org/10.7717/peerj.8667</a>

431 432 433	22	Oxenford, H. A., Cox, SA., van Tussenbroek, B. I. & Desrochers, A. Challenges of Turning the <i>Sargassum</i> Crisis into Gold: Current Constraints and Implications for the Caribbean. <i>Phycology</i> <b>1</b> , 27-48 (2021).
434 435 436	23	Devault, D. A. et al. The silent spring of Sargassum. Environmental Science and Pollution Research 28, 15580-15583 (2021). <a href="https://doi.org/10.1007/s11356-020-12216-7">https://doi.org/10.1007/s11356-020-12216-7</a>
437 438	24	Smetacek, V. & Zingone, A. Green and golden seaweed tides on the rise. <i>Nature</i> <b>504</b> , 84-88 (2013). <a href="https://doi.org:10.1038/nature12860">https://doi.org:10.1038/nature12860</a>
439 440 441	25	Schell, J. M., Goodwin, D. S. & Siuda, A. N. S. Recent <i>Sargassum</i> Inundation Events in the Caribbean: Shipboard Observations Reveal Dominance of a Previously Rare Form. <i>Oceanography</i> <b>28</b> , 8-11 (2015).
442 443	26	Wang, M. <i>et al.</i> The great Atlantic <i>Sargassum</i> belt. <i>Science</i> <b>365</b> , 83-87 (2019). <a href="https://doi.org:10.1126/science.aaw7912">https://doi.org:10.1126/science.aaw7912</a>
444 445 446 447	27	Johns, E. M. <i>et al.</i> The establishment of a pelagic <i>Sargassum</i> population in the tropical Atlantic: Biological consequences of a basin-scale long distance dispersal event. <i>Progress in Oceanography</i> <b>182</b> , 102269 (2020). <a href="https://doi.org/10.1016/j.pocean.2020.102269">https://doi.org/10.1016/j.pocean.2020.102269</a>
448 449 450 451	28	Oviatt, C. A., Huizenga, K., Rogers, C. S. & Miller, W. J. What nutrient sources support anomalous growth and the recent <i>Sargassum</i> mass stranding on Caribbean beaches? A review. <i>Marine Pollution Bulletin</i> <b>145</b> , 517-525 (2019). <a href="https://doi.org/10.1016/j.marpolbul.2019.06.049">https://doi.org/10.1016/j.marpolbul.2019.06.049</a>
452 453 454	29	Lapointe, B. E. <i>et al.</i> Nutrient content and stoichiometry of pelagic <i>Sargassum</i> reflects increasing nitrogen availability in the Atlantic Basin. <i>Nature Communications</i> <b>12</b> , 3060 (2021). <a href="https://doi.org:10.1038/s41467-021-23135-7">https://doi.org:10.1038/s41467-021-23135-7</a>
455 456 457	30	Parr, A. E. Quantitative Observations on the Pelagic <i>Sargassum</i> Vegetation of the Western North Atlantic: With Preliminary Discussion of Morphology and Relationships. <i>Bull. Bingham Oceanogr. Collect.</i> <b>6</b> , 1-94 (1939).
458 459 460	31	Putman, N. F. <i>et al.</i> Simulating transport pathways of pelagic <i>Sargassum</i> from the Equatorial Atlantic into the Caribbean Sea. <i>Progress in Oceanography</i> <b>165</b> , 205-214 (2018). <a href="https://doi.org/10.1016/j.pocean.2018.06.009">https://doi.org/10.1016/j.pocean.2018.06.009</a>
461 462	32	Beron-Vera, F. J. <i>et al.</i> Dynamical geography and transition paths of <i>Sargassum</i> in the tropical Atlantic. <i>AIP Advances</i> <b>12</b> , 105107 (2022). <a href="https://doi.org:10.1063/5.0117623">https://doi.org:10.1063/5.0117623</a>
463 464	33	van Sebille, E. <i>et al.</i> Dispersion of Surface Drifters in the Tropical Atlantic. <i>Frontiers in Marine Science</i> <b>7</b> (2021). <a href="https://doi.org:10.3389/fmars.2020.607426">https://doi.org:10.3389/fmars.2020.607426</a>

465 466 467	34	Montoya, J. P. in <i>Nitrogen in the Marine Environment (Second Edition)</i> (eds Douglas G. Capone, Deborah A. Bronk, Margaret R. Mulholland, & Edward J. Carpenter) 1277-1302 (Academic Press, 2008).
468 469	35	Carpenter, E. J. Nitrogen Fixation by a Blue-Green Epiphyte on Pelagic Sargassum. <i>Science</i> <b>178</b> , 1207-1209 (1972). <a href="https://doi.org/10.1126/science.178.4066.1207">https://doi.org/10.1126/science.178.4066.1207</a>
470 471 472	36	Carpenter, E. J. & Cox, J. L. Production of pelagic <i>Sargassum</i> and a blue-green epiphyte in the western Sargasso Sea. <i>Limnology and Oceanography</i> <b>19</b> , 429-436 (1974). <a href="https://doi.org/10.4319/lo.1974.19.3.0429">https://doi.org/10.4319/lo.1974.19.3.0429</a>
473 474 475	37	Kendall, C., Elliott, E. M. & Wankel, S. D. in <i>Stable Isotopes in Ecology and Environmental Science</i> (eds R. Michener & K. Lajtha) Ch. 12, 375-449 (Blackwell Publishing, 2007).
476 477 478	38	Gower, J. & King, S. Satellite Images Show the Movement of Floating <i>Sargassum</i> in the Gulf of Mexico and Atlantic Ocean. <i>Nature Precedings</i> (2008). <a href="https://doi.org:10.1038/npre.2008.1894.1">https://doi.org:10.1038/npre.2008.1894.1</a>
479 480 481	39	Hu, C. <i>et al.</i> Mississippi River water in the Florida Straits and in the Gulf Stream off Georgia in summer 2004. <i>Geophysical Research Letters</i> <b>32</b> (2005). <a href="https://doi.org/10.1029/2005GL022942">https://doi.org/10.1029/2005GL022942</a>
482 483 484	40	Magaña-Gallegos, E. <i>et al.</i> Growth rates of pelagic <i>Sargassum</i> species in the Mexican Caribbean. <i>Aquatic Botany</i> <b>185</b> , 103614 (2023). <a href="https://doi.org/10.1016/j.aquabot.2022.103614">https://doi.org/10.1016/j.aquabot.2022.103614</a>
485 486	41	Hanisak, M. D. & Samuel, M. A. in <i>Twelfth International Seaweed Symposium</i> . (eds Mark A. Ragan & Carolyn J. Bird) 399-404 (Springer Netherlands).
487 488 489 490	42	Knapp, A. N., DiFiore, P. J., Deutsch, C., Sigman, D. M. & Lipschultz, F. Nitrate isotopic composition between Bermuda and Puerto Rico: Implications for N <sub>2</sub> fixation in the Atlantic Ocean. <i>Global Biogeochemical Cycles</i> <b>22</b> , 1-14 (2008). <a href="https://doi.org:10.1029/2007gb003107">https://doi.org:10.1029/2007gb003107</a>
491 492 493	43	Knapp, A. N., Sigman, D. M. & Lipschultz, F. N isotopic composition of dissolved organic nitrogen and nitrate at the Bermuda Atlantic Time-series Study site. <i>Global Biogeochemical Cycles</i> <b>19</b> (2005). <a href="https://doi.org/10.1029/2004GB002320">https://doi.org/10.1029/2004GB002320</a>
494 495 496	44	Gower, J., Young, E. & King, S. Satellite images suggest a new <i>Sargassum</i> source region in 2011. <i>Remote Sensing Letters</i> <b>4</b> , 764-773 (2013). <a href="https://doi.org:10.1080/2150704X.2013.796433">https://doi.org:10.1080/2150704X.2013.796433</a>
497 498 499 500	45	Lapointe, B. E. Phosphorus-limited photosynthesis and growth of <i>Sargassum natans</i> and <i>Sargassum fluitans</i> (Phaeophyceae) in the western North Atlantic. <i>Deep Sea Research Part A. Oceanographic Research Papers</i> <b>33</b> , 391-399 (1986). <a href="https://doi.org/10.1016/0198-0149(86)90099-3">https://doi.org/10.1016/0198-0149(86)90099-3</a>

501 502 503	46	Benson, A. A., Katayama, M. & Knowles, F. C. Arsenate metabolism in aquatic plants. <i>Applied Organometallic Chemistry</i> <b>2</b> , 349-352 (1988). <a href="https://doi.org/10.1002/aoc.590020411">https://doi.org/10.1002/aoc.590020411</a>
504 505 506	47	Sanders, J. G. The concentration and speciation of arsenic in marine macro-algae. <i>Estuarine and Coastal Marine Science</i> <b>9</b> , 95-99 (1979). <a href="https://doi.org/10.1016/0302-3524(79)90010-0">https://doi.org/10.1016/0302-3524(79)90010-0</a>
507 508 509 510	48	Cutter, G. A., Cutter, L. S., Featherstone, A. M. & Lohrenz, S. E. Antimony and arsenic biogeochemistry in the western Atlantic Ocean. <i>Deep Sea Research Part II: Topical Studies in Oceanography</i> <b>48</b> , 2895-2915 (2001). <a href="https://doi.org/10.1016/S0967-0645(01)00023-6">https://doi.org/10.1016/S0967-0645(01)00023-6</a>
511 512 513	49	Wurl, O., Zimmer, L. & Cutter, G. A. Arsenic and phosphorus biogeochemistry in the ocean: Arsenic species as proxies for P-limitation. <i>Limnology and Oceanography</i> <b>58</b> , 729-740 (2013). <a href="https://doi.org/10.4319/lo.2013.58.2.0729">https://doi.org/10.4319/lo.2013.58.2.0729</a>
514 515 516 517	50	Mamun, M. A. A. <i>et al.</i> Bioaccumulation and biotransformation of arsenic by the brown macroalga <i>Sargassum patens</i> C. Agardh in seawater: effects of phosphate and iron ions. <i>Journal of Applied Phycology</i> <b>31</b> , 2669-2685 (2019). <a href="https://doi.org.10.1007/s10811-018-1721-x">https://doi.org.10.1007/s10811-018-1721-x</a>
518 519 520	51	Sanders, J. G. & Windom, H. L. The uptake and reduction of arsenic species by marine algae. <i>Estuarine and Coastal Marine Science</i> <b>10</b> , 555-567 (1980). <a href="https://doi.org/10.1016/S0302-3524(80)80075-2">https://doi.org/10.1016/S0302-3524(80)80075-2</a>
521 522 523 524	52	Gobert, T. <i>et al.</i> Trace metal content from holopelagic <i>Sargassum</i> spp. sampled in the tropical North Atlantic Ocean: Emphasis on spatial variation of arsenic and phosphorus. <i>Chemosphere</i> <b>308</b> , 136186 (2022). <a href="https://doi.org/10.1016/j.chemosphere.2022.136186">https://doi.org/10.1016/j.chemosphere.2022.136186</a>
525 526 527 528	53	Lapointe, B. E. A comparison of nutrient-limited productivity in <i>Sargassum natans</i> from neritic vs. oceanic waters of the western North Atlantic Ocean. <i>Limnology and Oceanography</i> <b>40</b> , 625-633 (1995). <a href="https://doi.org/10.4319/lo.1995.40.3.0625">https://doi.org/10.4319/lo.1995.40.3.0625</a>
529 530	54	Woosley, R. & Thurnherr, A. M. Hydrographic data from voyage TN389 of the R/V <i>Thomas G. Thompson</i> . <a href="https://cchdo.ucsd.edu/cruise/325020210316">https://cchdo.ucsd.edu/cruise/325020210316</a> (2021).
531 532	55	Menezes, V. & Anderson, J. Hydrographic data from voyage TN390 of the R/V <i>Thomas G. Thompson</i> . <a href="https://cchdo.ucsd.edu/cruise/325020210420">https://cchdo.ucsd.edu/cruise/325020210420</a> (2021).
533 534 535	56	Becker, S. et al. in GO-SHIP Repeat Hydrography Manual: A Collection of Expert Reports and Guidelines <a href="https://www.go-ship.org/HydroMan.html">https://www.go-ship.org/HydroMan.html</a> (GO-SHIP Program and SCOR, 2019).

536 537 538	57	Dibner, S. <i>et al.</i> Consistent genetic divergence observed among pelagic <i>Sargassum</i> morphotypes in the western North Atlantic. <i>Marine Ecology</i> <b>43</b> , e12691 (2022). <a href="https://doi.org/10.1111/maec.12691">https://doi.org/10.1111/maec.12691</a>
539 540 541 542	58	Amaral-Zettler, L. A. <i>et al.</i> Comparative mitochondrial and chloroplast genomics of a genetically distinct form of <i>Sargassum</i> contributing to recent "Golden Tides" in the Western Atlantic. <i>Ecology and evolution</i> <b>7</b> , 516-525 (2016). <a href="https://doi.org:10.1002/ece3.2630">https://doi.org:10.1002/ece3.2630</a>
543 544	59	Allen, S. E., Grimshaw, H. M., Parkinson, J. A., Quarmby, C. & Roberts, J. D. <i>Chemical Analysis of Ecological Materials</i> . (Blackwell Scientific Publications, 1974).
545 546	60	Jones, J. B., Wolf, B. & Mills, H. A. in <i>Plant Analysis Handbook</i> 195-196 (Micro-Macro Publishing, 1990).
547 548	61	Kelly, T. B. TheSource: An R library of simple utilities to facilitate research (V0.1.6). <i>Zenodo</i> (2019). <a href="https://doi.org/10.5281/zenodo.3468524">https://doi.org/10.5281/zenodo.3468524</a>
549 550 551 552	62	Cole, S. T., Wortham, C., Kunze, E. & Owens, W. B. Eddy stirring and horizontal diffusivity from Argo float observations: Geographic and depth variability. <i>Geophysical Research Letters</i> <b>42</b> , 3989-3997 (2015). <a href="https://doi.org/10.1002/2015GL063827">https://doi.org/10.1002/2015GL063827</a>
553 554 555	63	Berline, L. <i>et al.</i> Hindcasting the 2017 dispersal of <i>Sargassum</i> algae in the Tropical North Atlantic. <i>Marine Pollution Bulletin</i> <b>158</b> , 111431 (2020). <a href="https://doi.org/10.1016/j.marpolbul.2020.111431">https://doi.org/10.1016/j.marpolbul.2020.111431</a>
556 557 558	64	Putman, N. F., Lumpkin, R., Olascoaga, M. J., Trinanes, J. & Goni, G. J. Improving transport predictions of pelagic <i>Sargassum. Journal of Experimental Marine Biology and Ecology</i> <b>529</b> , 151398 (2020). <a href="https://doi.org/10.1016/j.jembe.2020.151398">https://doi.org/10.1016/j.jembe.2020.151398</a>
559 560 561	65	Kalnay, E. <i>et al.</i> The NCEP/NCAR 40-Year Reanalysis Project. <i>Bulletin of the American Meteorological Society</i> <b>77</b> , 437-472 (1996). <a href="https://doi.org/10.1175/1520-0477(1996)077">https://doi.org/10.1175/1520-0477(1996)077</a> <0437:TNYRP>2.0.CO;2
562 563 564	66	Wang, M. & Hu, C. Mapping and quantifying <i>Sargassum</i> distribution and coverage in the Central West Atlantic using MODIS observations. <i>Remote Sensing of Environment</i> <b>183</b> , 350-367 (2016). <a href="https://doi.org/10.1016/j.rse.2016.04.019">https://doi.org/10.1016/j.rse.2016.04.019</a>
565 566 567 568 569	67	Hu, C. A novel ocean color index to detect floating algae in the global oceans. <i>Remote Sensing of Environment</i> <b>113</b> , 2118-2129 (2009). <a href="https://doi.org/10.1016/j.rse.2009.05.012">https://doi.org/10.1016/j.rse.2009.05.012</a>

- 570 **Acknowledgments**
- 571 Sargassum samples of opportunity were collected on U.S. GO-SHIP lines A20 (Ryan Woosley,
- 572 Chief Scientist), and A22 (Vivienne Menezes, Chief Scientist), carried out on the R/V Thomas
- 573 G. Thompson (voyages TN389 and TN390) with the support of NSF and NOAA. We greatly
- 574 appreciate the efforts of all who participated in the collection, processing, and preservation of the
- 575 samples on these cruises, particularly Christine Klimkowski, Jennifer Nomura, Elizabeth Ricci,
- 576 and Stephen Jalickee. Likewise, we thank Kevin Tyre, Allyson DiMarco, Dave Milmore, and
- 577 Kristie Dick for their efforts processing cruise samples.

- 579 D.J.M. gratefully acknowledges partial support of this effort by the National Science Foundation
- 580 (Grant Number OCE-1840381) and the National Institute of Environmental Health Sciences
- 581 (Grant Number 1P01ES028938) through the Woods Hole Center for Oceans and Human Health,
- 582 as well as internal support provided by the Woods Hole Oceanographic Institution and the Isham
- 583 Family Charitable Fund. D.J.M. thanks O. Kosnyrev for her skillful data analysis and
- 584 visualization.

585

- 586 C.H., R.A.B., and B.E.L. acknowledge the support of the National Aeronautics and Space
- Administration (Grant Number 80NSSC20M0264). 587

588

589 We thank Yingjun Zhang for the SMOS salinity analysis that went into Figure 1.

590

- 591 A portion of P. Morton's work was performed at the National High Magnetic Field Laboratory, 592 which is supported by National Science Foundation Cooperative Agreement No. DMR-1644779
- 593 and the State of Florida.

594 595

596

- **Author contributions** 597 The following uses categories defined at: https://www.elsevier.com/authors/policies-and-
- 598 guidelines/credit-author-statement

599

- 600 D.J.M. Conceptualization, methodology, formal analysis, investigation, writing-601 original draft, writing-reviewing and editing.
- 602 R.A.B. Data curation, writing - review and editing.
- 603 C.H. Investigation, writing - review and editing.
- 604 T.B.K. Investigation, writing - review and editing.
- 605 P.L.M. Investigation, resources, writing – review and editing.
- 606 A.R.S. Formal analysis, writing – review and editing.
- 607 B.E.L. Conceptualization, methodology, investigation, writing-reviewing and editing.

- 609 **Competing Interests**
- 610 The authors declare no competing interests.

# **Figures**

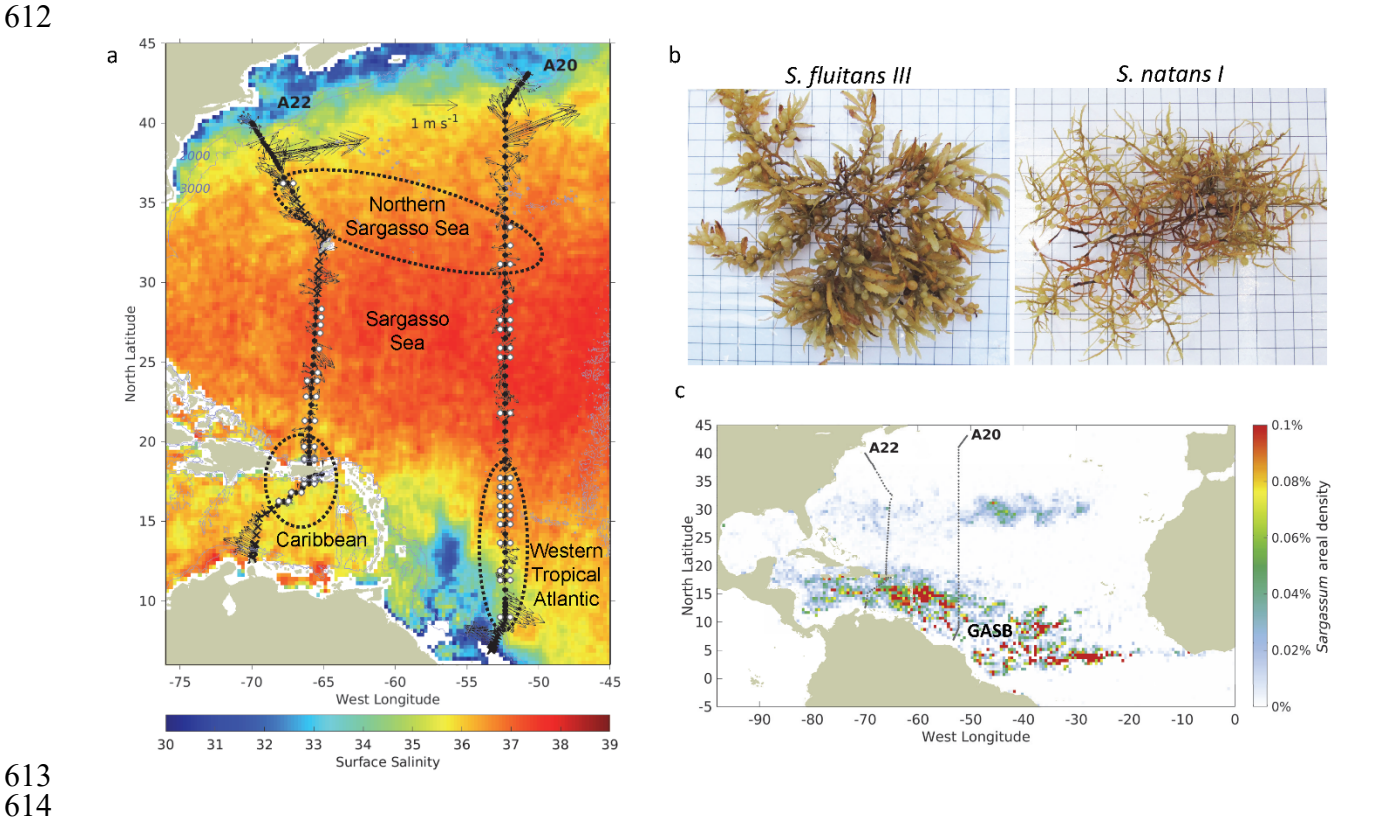


**Fig. 1.** Sargassum sampling on GO-SHIP lines A20 (16 March – 16 April 2021) and A22 (20 April – 16 May 2021). a, White circles indicate collection of Sargassum samples, with S. fluitans III shown to the left and S. natans I to the right of the station locations, which are indicated as black circles (where Sargassum sampling was possible), and black Xs (where Sargassum sampling was not possible). Dashed black lines indicate sample groupings in the northern Sargasso Sea, Sargasso Sea, western tropical Atlantic, and Caribbean. Velocity vectors are from the uppermost bin (centered at 29 m depth) of the ship's ADCP. The surface salinity field is comprised of a time-average of SMOS measurements for the cruise period (16 March – 16 May, 2021). b, Photographs of S. fluitans III and S. natans I samples on a 1 cm grid background. Photo credit: Amy Siuda and Jeffrey Schell, Sea Education Association. c, Location of GO-SHIP lines A20 and A22 relative to the GASB (contiguous area of Sargassum coverage surrounding the annotation) for the cruise period estimated from MODIS data. Blue lines are the 2000 m and 3000 m isobaths.

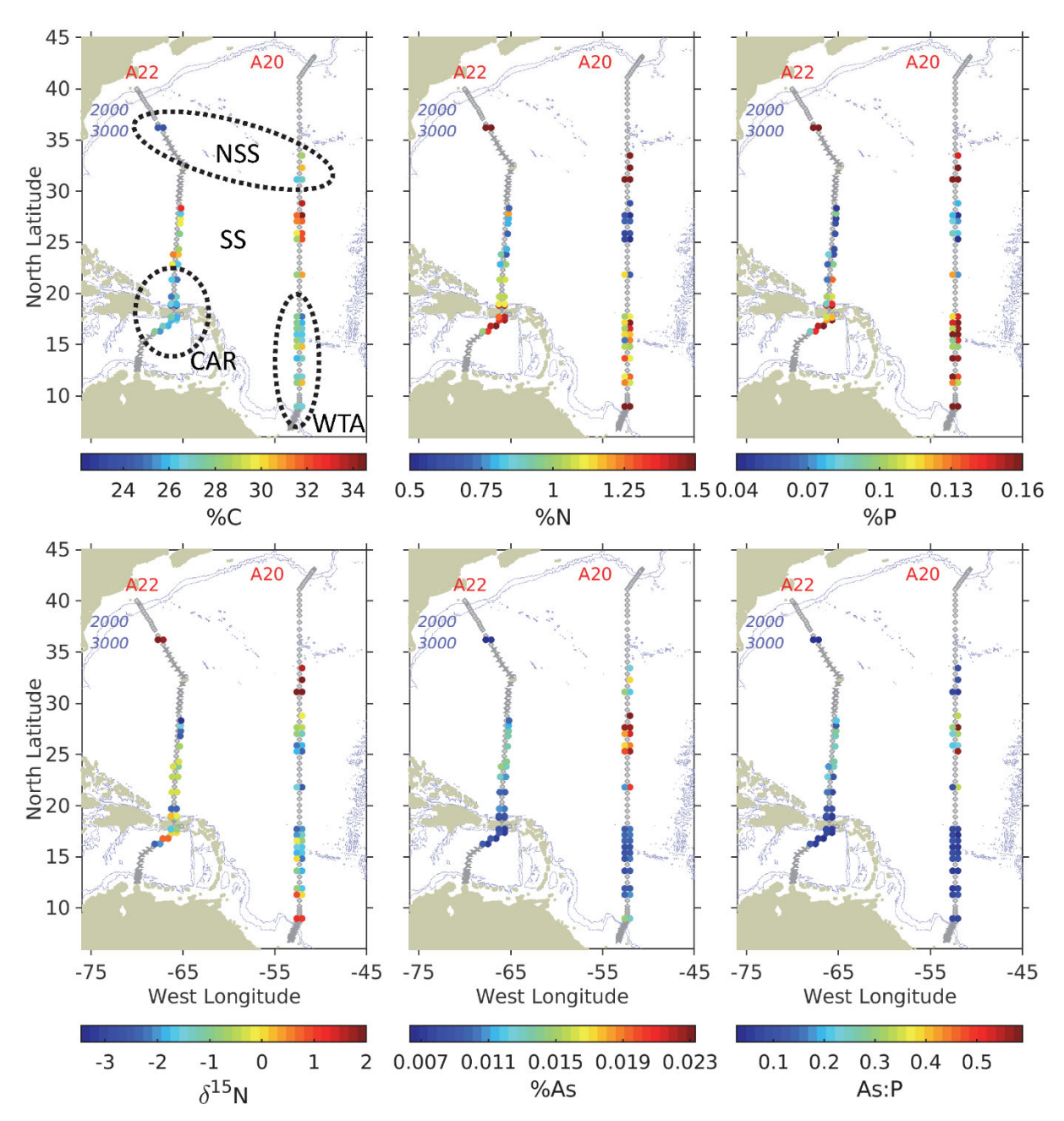
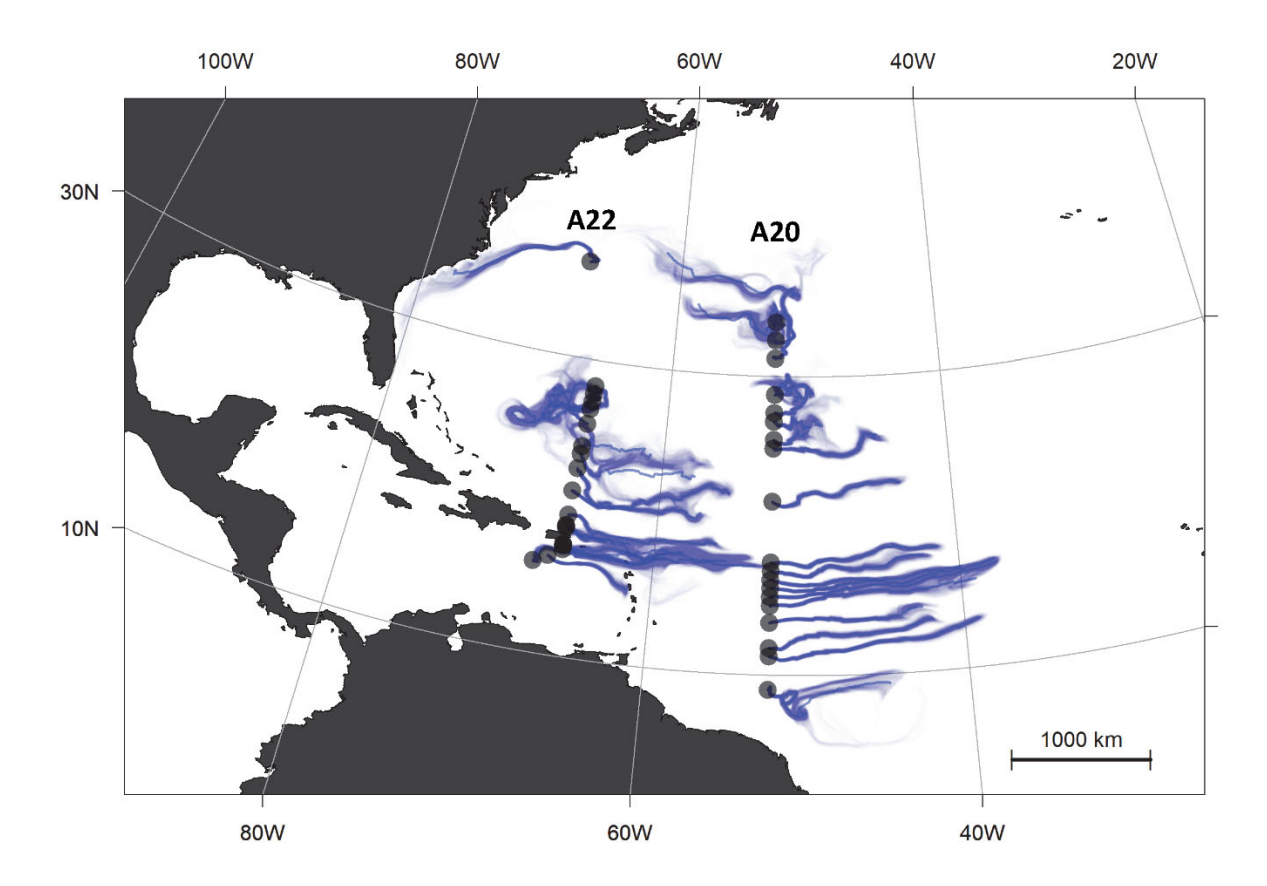
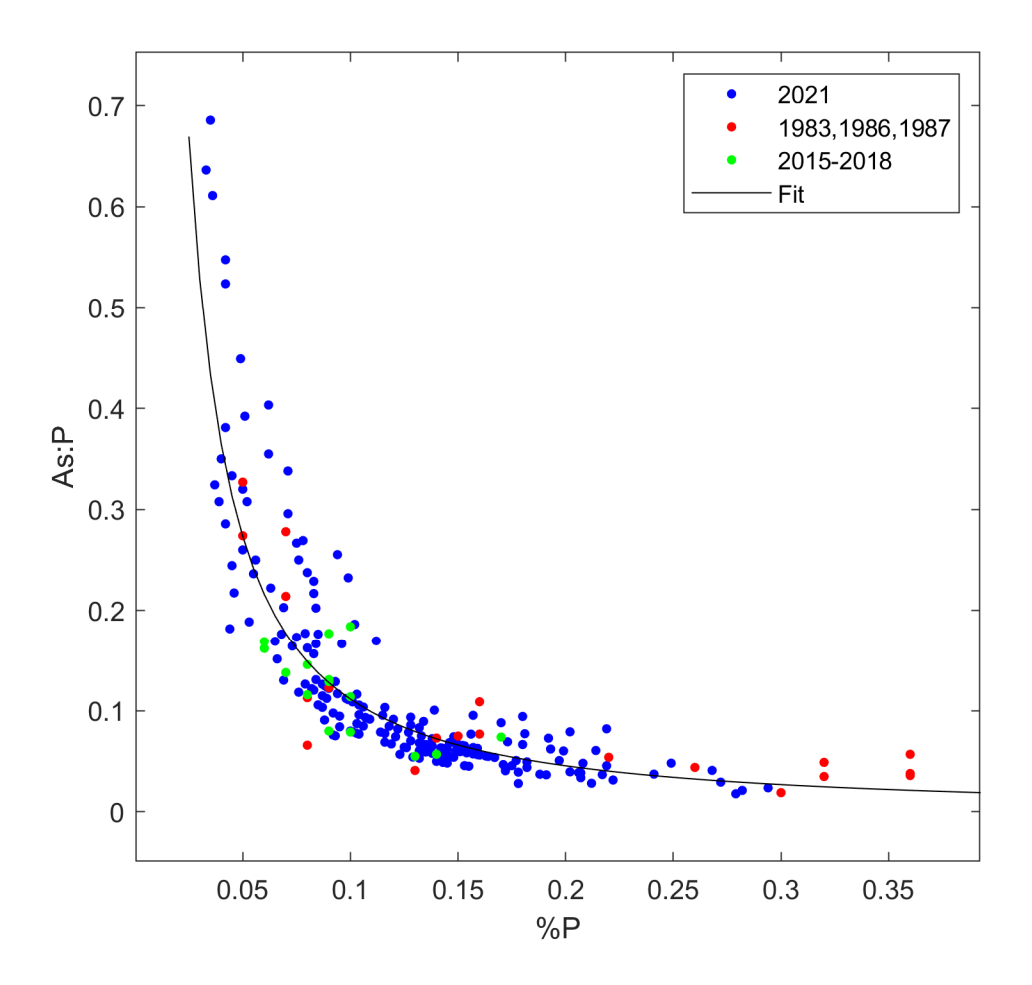


Fig. 2. Sargassum tissue data: Top row: carbon (left), nitrogen (middle), and phosphorus (right) content (% dry weight). Bottom row:  $\delta^{15}$ N values, arsenic content, and arsenic to phosphorus ratio in Sargassum tissue. S. fluitans III is shown to the left of transects A20 and A22, and S. natans I to the right. Stations where no Sargassum was found are shown as circles, and stations where Sargassum sampling was not possible are shown as Xs. Dashed black lines in the upper left panel indicate sample groupings in Northern Sargasso Sea (NSS), Sargasso Sea (SS), Caribbean (CAR), and Western Tropical Atlantic (WTA), as in Fig. 1. Blue lines are the 2000 m and 3000 m isobaths.



**Fig. 3. Origins of** *Sargassum* **spp. samples from GO-SHIP lines A20 and A22**. Surface particles deployed at sample collection sites (Figs. 1 and 2) were tracked back in time for 60 days. The centroid of the ensemble is shown as a bold blue line with individual trajectories shown in lighter blue.



**Fig. 4.** Arsenic to phosphorus ratio as a function of phosphorus content in *Sargassum* tissue. Data from GO-SHIP lines A20 and A22 in 2021 are in blue (N=200), 1983-1987 in red (N=20), and 2015-2018 in green (N=21). Black line is the fit described in the Supplementary Note.

## **Supplementary Information**

 Supplementary Table 1. Subregional comparisons of elemental composition (% dry weight) and ratios, as well as stable isotope values (‰) for *S. fluitans* and *S. natans*. Mean and 95% confidence interval are indicated in each case. See Fig. 1 for geographic boundaries of the subregions.

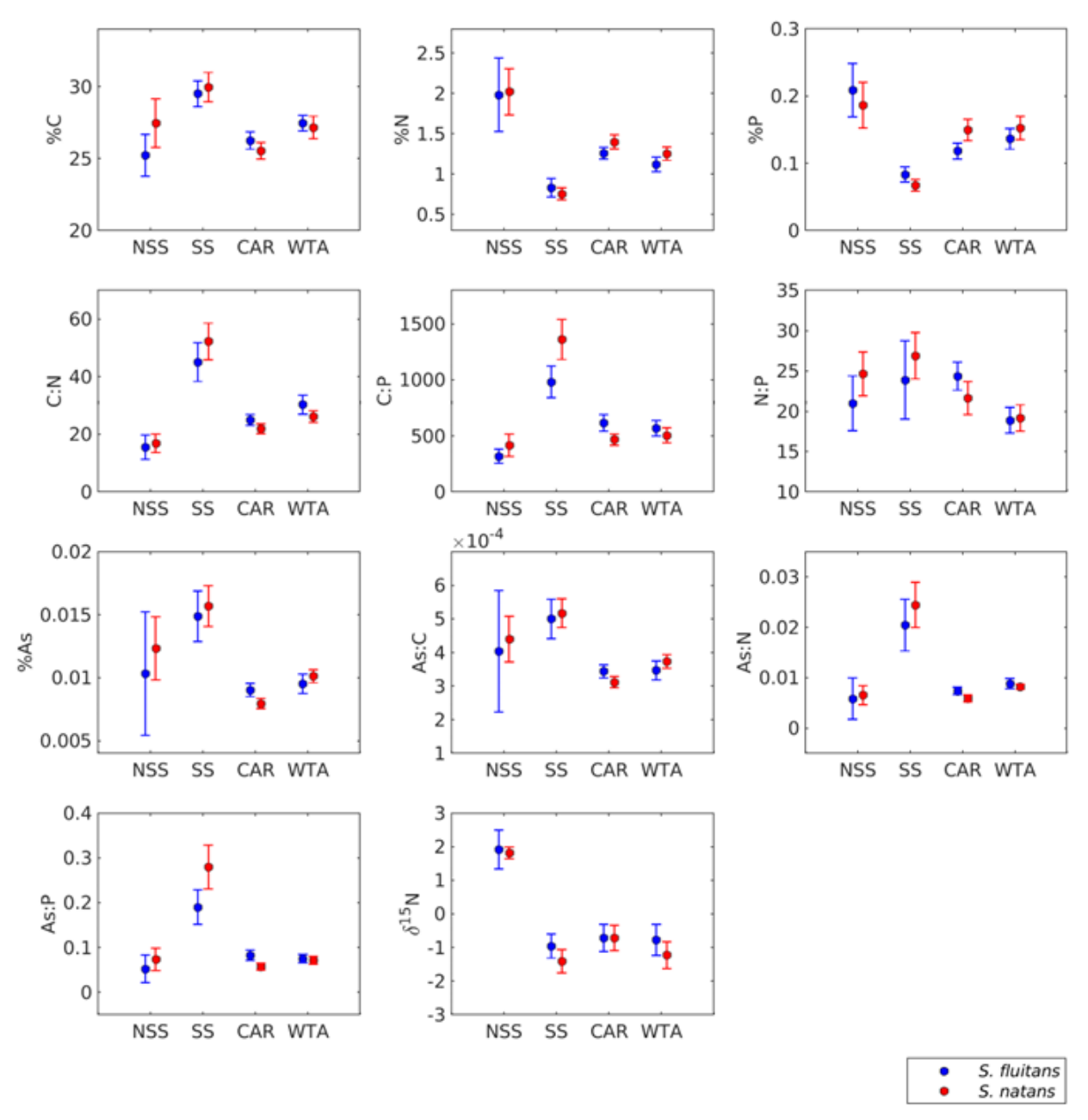
	Northern Sa	argasso Sea	Sargasso Sea		Carib	bean	Western Tropical		
							Atlantic		
	S. fluitans	S. natans	S. fluitans S. natans		S. fluitans S. natans		S. fluitans	S. natans	
N	6	12	20	43	30	29	30	30	
%C	$25.2 \pm 1.5$	$27.5 \pm 1.7$	$29.5 \pm 0.9$	$30.0\pm1.0$	$26.3\pm0.6$	$25.6 \pm 0.6$	$27.5 \pm 0.5$	$27.2 \pm 0.8$	
%N	$2.0\pm0.5$	$2.0 \pm 0.3$	$0.8 \pm 0.1$	$0.8 \pm 0.1$	$1.3 \pm 0.1$	$1.4 \pm 0.1$	$1.1 \pm 0.1$	$1.3 \pm 0.1$	
%P	$0.21\pm0.04$	$0.19 \pm 0.03$	$0.08\pm0.01$	$0.07 \pm 0.01$	$0.12\pm0.01$	$0.15\pm0.02$	$0.14 \pm 0.02$	$0.15\pm0.02$	
C:N	$15.6 \pm 4.3$	$16.9 \pm 3.2$	$45.1 \pm 6.7$	$52.3 \pm 6.4$	$25.1 \pm 1.8$	$22.0 \pm 1.7$	$30.4 \pm 3.3$	$26.2\pm2.0$	
C:P	$320\pm63$	$419\pm100$	$984 \pm 142$	$1363 \pm 179$	$619 \pm 74$	$469 \pm 49$	$570 \pm 71$	$506 \pm 67$	
N:P	$21.0 \pm 3.4$	$24.7 \pm 2.7$	$23.9 \pm 4.8$	$26.9 \pm 2.9$	$24.4\pm1.7$	$21.6 \pm 2.0$	$18.9 \pm 1.6$	$19.2 \pm 1.6$	
$\delta^{15}N$	$1.93 \pm 0.58$	$1.82 \pm 0.18$	$-0.95 \pm 0.36$	$-1.40 \pm 0.34$	$-0.71 \pm 0.41$	$-0.71 \pm 0.37$	$-0.77 \pm 0.46$	$-1.22 \pm 0.40$	
%As	0.010 ± 0.005	0.012 ± 0.003	0.015 ± 0.002	0.016 ± 0.002	0.009 ± 0.001	$0.008 \pm 0.0004$	0.010 ± 0.001	0.010 ± 0.001	

Supplementary Table 2. Statistical significance (p-values of two-sided t-tests) for subregional comparisons of mean elemental composition, stoichiometry, and stable isotope values for the combined species *S. fluitans* and *S. natans*. Cells with p-values in excess of 0.05 are highlighted. See Fig. 1 for geographic boundaries of sample groupings in the Northern Sargasso Sea (NSS), Sargasso Sea (SS), Caribbean (CAR), and Western Tropical Atlantic (WTA).

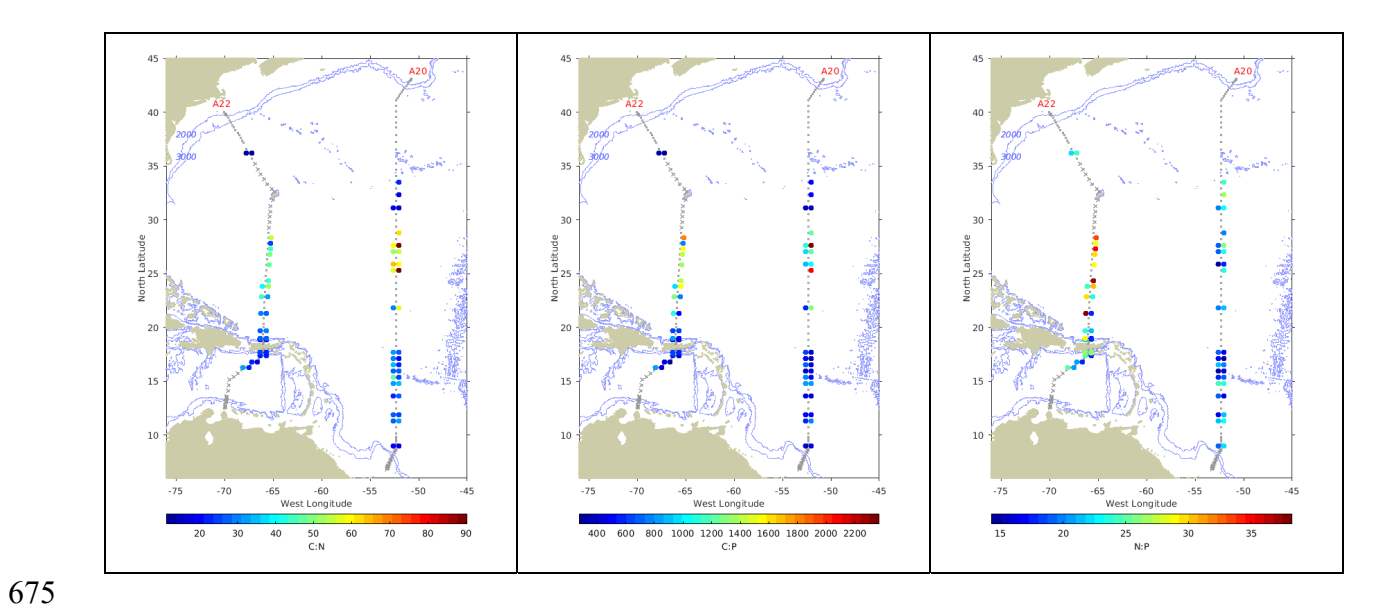
%C	SS	CAR	WTA	%N	SS	CAR	WTA	%P	SS	CAR	WTA
NSS	1.03e-04	0.21	0.36		2.40e-10	2.94e-06	1.79e-07		2.53e-09	7.82e-05	7.19e-04
SS		6.94e-15	1.08e-07			3.88e-25	4.20e-16			1.56e-16	2.91e-18
CAR			1.33e-05				9.80e-04				0.17
C:N				C:P				N:P			
NSS	1.10e-20	4.42e-06	2.31e-10		3.87e-18	3.55e-04	6.10e-04		0.11	0.74	6.72e-04
SS		2.65e-16	1.29e-12			7.24e-15	4.68e-15			0.04	1.46e-06
CAR			1.03e-04				0.83				1.24e-05
%As				As:C				As:N			
NSS	2.73e-03	5.38e-03	0.09		0.02	4.50e-03	0.04		1.12e-13	0.68	0.01
SS		1.27e-16	9.99e-13			4.01e-16	3.36e-12			6.11e-14	4.70e-12
CAR			9.62e-06				3.67e-03				4.03e-06
As:P				$\delta^{15}N$							
NSS	6.58e-14	0.74	0.48		2.74e-31	1.91e-25	1.59e-26				
SS		2.28e-14	4.74e-14			3.88e-03	0.19				
CAR			0.49				0.16				

Supplementary Table 3. Summary of least squares fits y = ax + b for arsenic content as a function of phosphorus, nitrogen, and carbon content (% dry weight). Asterisk indicates p-values so low that they could not be distinguished from zero.

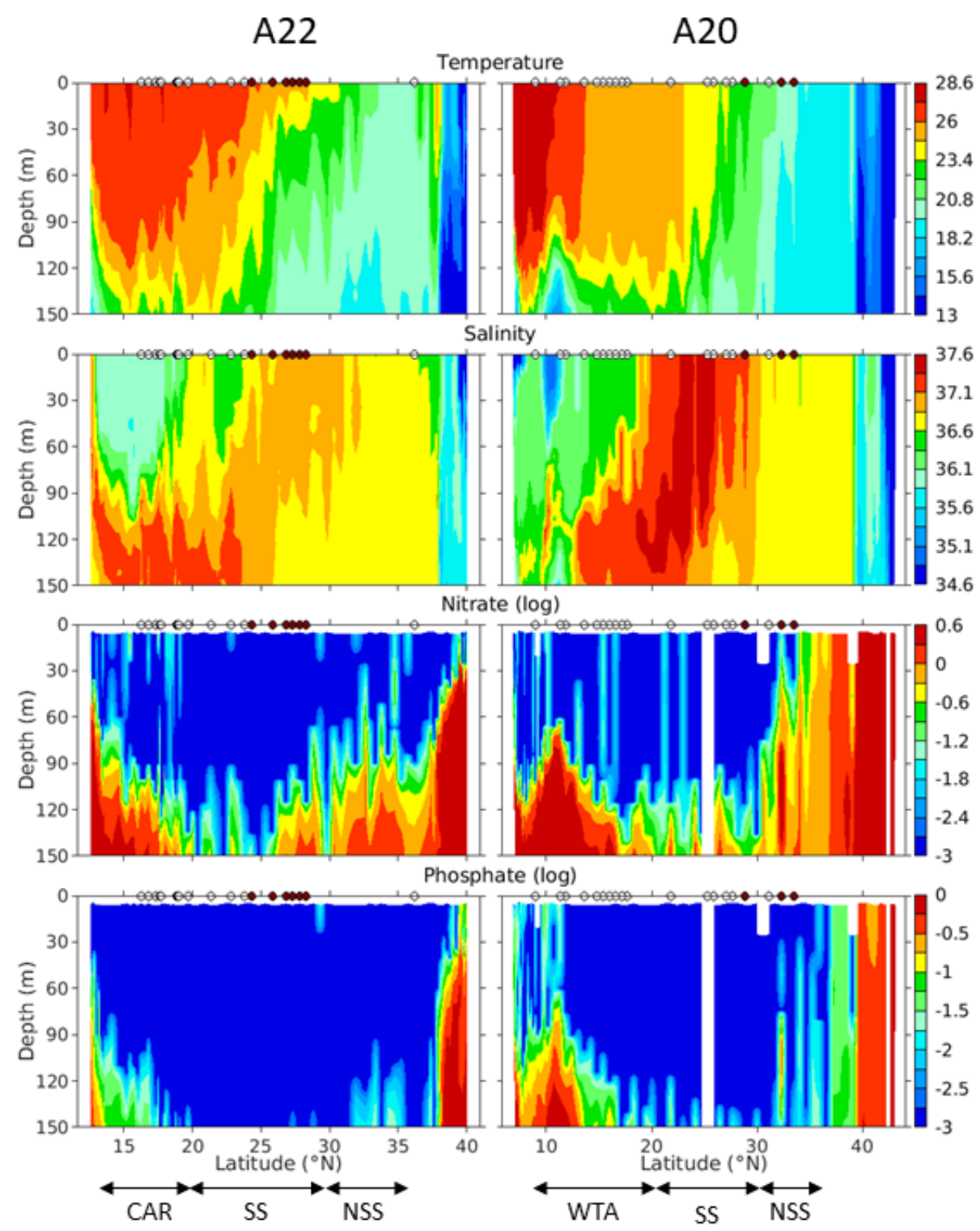
у	X	$r^2$	Intercept (b)	р	Slope (a)	р
As	P	0.23	1.60e-02	0.00e+00*	-3.79e-02	1.16e-12
As	N	0.27	1.75e-02	0.00e+00*	-5.25e-03	3.66e-15
As	С	0.50	-1.98e-02	3.33e-16	1.13e-03	0.00e+00*



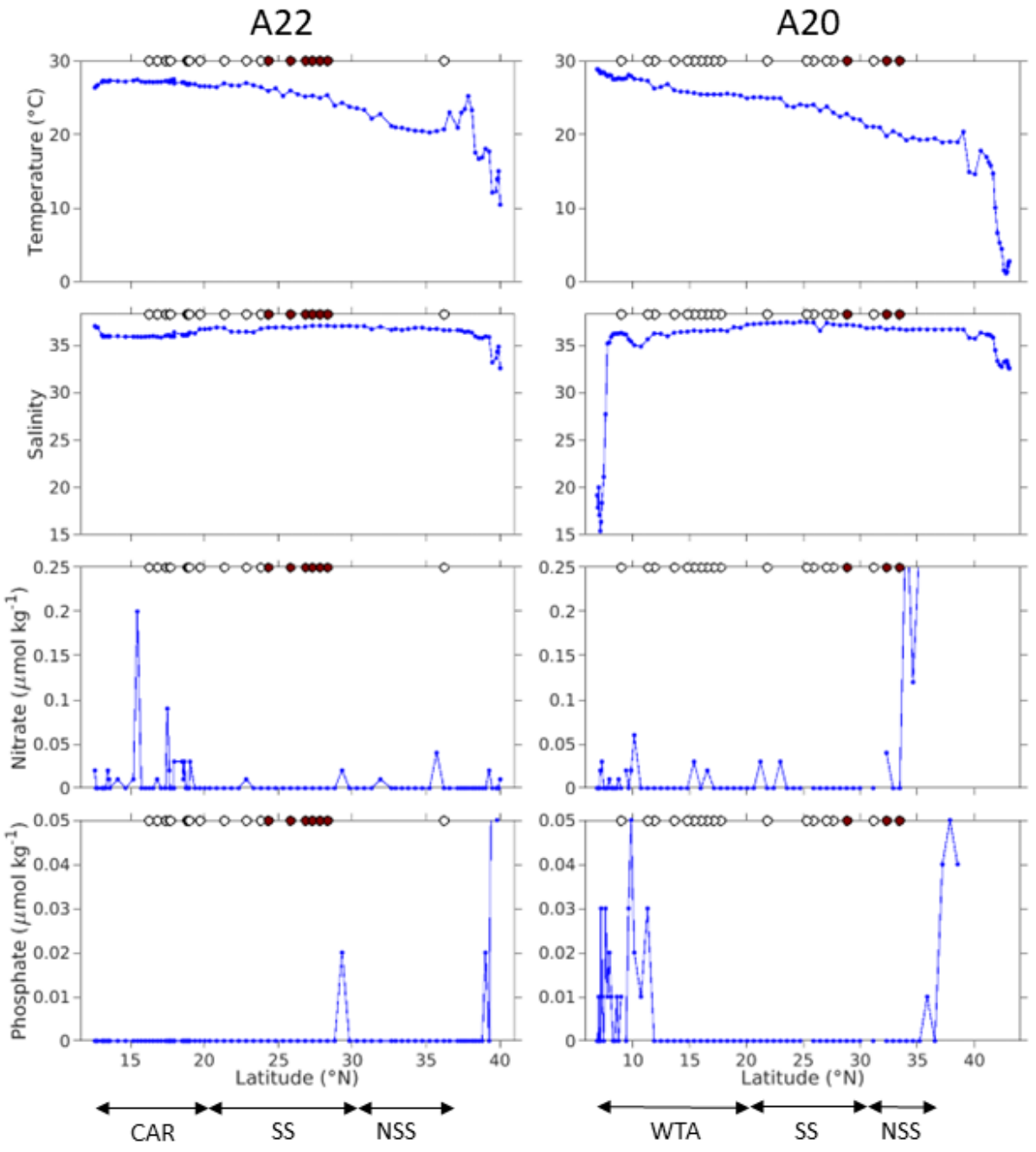
Supplementary Fig. 1. Subregional comparisons (by species) of carbon, nitrogen, and phosphorus content (top row), elemental ratios (middle row and bottom left), and stable isotope values (bottom row, middle and right) for the Northern Sargasso Sea (NSS), Sargasso Sea (SS), Caribbean (CAR), and Western Tropical Atlantic (WTA). Error bars are 95% confidence intervals.



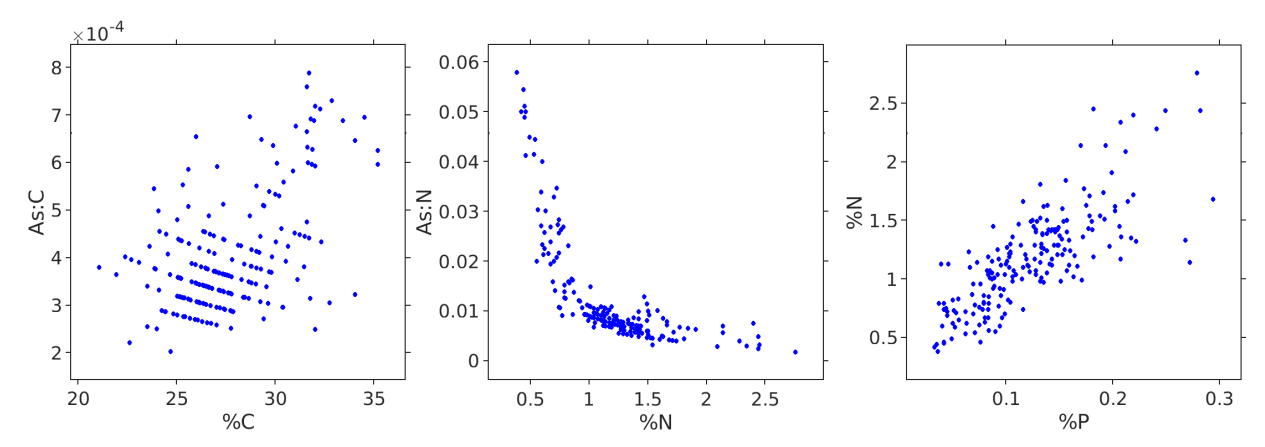
Supplementary Fig. 2. *Sargassum* elemental ratios: carbon to nitrogen (left), carbon to phosphorus (middle), and nitrogen to phosphorus (right). *S. fluitans III* is shown to the left of transects A20 and A22, and *S. natans I* to the right. Stations where no *Sargassum* was found are shown as circles, and stations where *Sargassum* sampling was not possible are shown as Xs. Blue lines are the 2000 m and 3000 m isobaths.



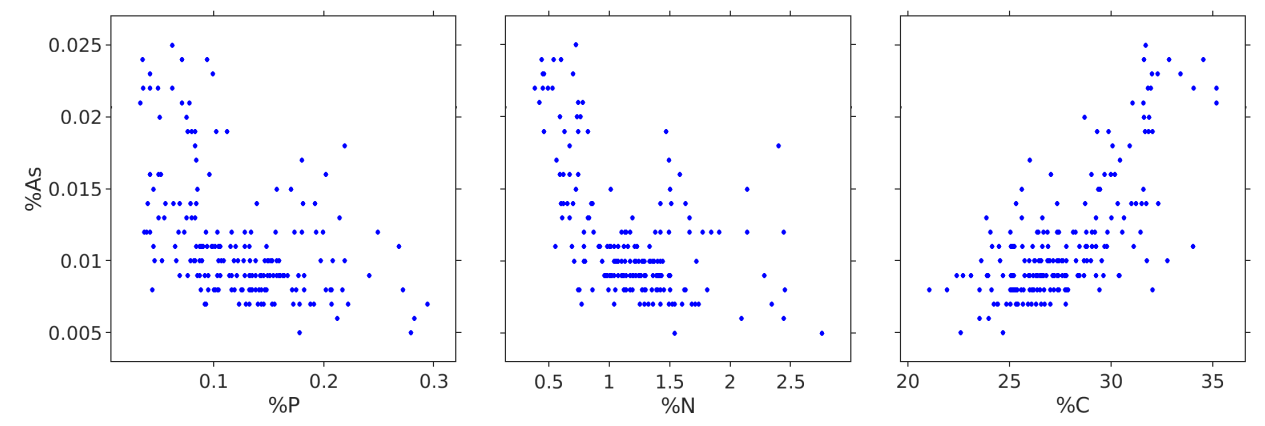
Supplementary Fig. 3. Vertical sections of temperature (°C), salinity, nitrate, and phosphate for A22 (left) and A20 (right). Nitrate and phosphate concentrations (µmol kg<sup>-1</sup>) have been log transformed in order to better resolve gradients at low concentrations. Circles along the top of each plot indicate stations where *Sargassum* was collected: *S. fluitans* and *S. natans* (white) and *S. natans* only (brown). Northern Sargasso Sea (NSS), Sargasso Sea (SS), Caribbean (CAR), and Western Tropical Atlantic (WTA) regions are indicated.



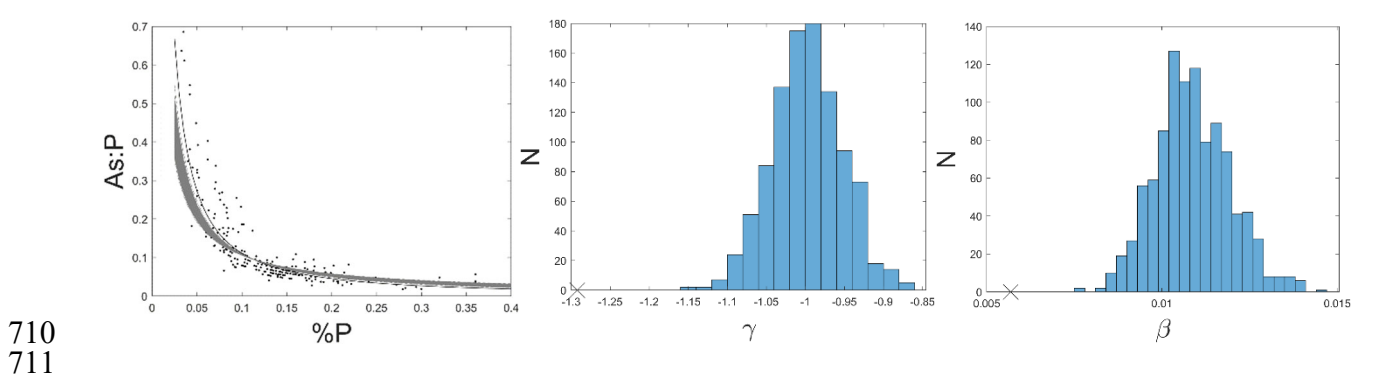
Supplementary Fig. 4. Surface temperature, salinity, nitrate, and phosphate for A22 (left) and A20 (right). Circles along the top of each plot indicate stations where *Sargassum* was collected: *S. fluitans* and *S. natans* (white) and *S. natans* only (brown). Northern Sargasso Sea (NSS), Sargasso Sea (SS), Caribbean (CAR), and Western Tropical Atlantic (WTA) regions are indicated.



Supplementary Fig. 5. Elemental ratios in *Sargassum* tissue. Left: arsenic to carbon ratio as a function of carbon content; middle: arsenic to nitrogen ratio as a function of nitrogen content; right: nitrogen content as a function of phosphorus content.



Supplementary Fig. 6. Arsenic in *Sargassum* tissue. Left: arsenic as a function of phosphorus content; middle: arsenic as a function of nitrogen content; right: arsenic content as a function of carbon content. Results of least squares fits are presented in Supplementary Table 3.



Supplementary Fig. 7. Left: Fits of the arsenic to phosphorus ratio in *Sargassum* ratio as a function of phosphorus content. Solid line is the fit to the data from Fig. 4 (black dots), and the gray lines are 1000 trials using the permuted phosphorus data as described in the Supplemental Note. Middle and left panels report the distribution of parameters  $\gamma$  and  $\beta$  for the permuted data (blue bars) and the actual data (X on the x-axes).

## **Supplementary Note**

The general model relating observations *i* of arsenic and phosphorus content we wish to test is

$$\frac{As_i}{P_i} = \beta P_i^{\gamma} \tag{1}$$

Where  $\gamma = -1$  would constitute the  $\frac{1}{p}$  dependence predicted by the theory. This model can be recast as

$$log(As_i) = c + (\gamma + 1)log(P_i)$$
 (2)

where  $c = log(\beta)$ . The parameters c and  $\gamma$  were estimated by least squares, and it turns out that the dependence of As:P on P is supra-hyperbolic:  $\gamma = -1.29 \pm 0.04$ . We tested the statistical robustness of this finding by permuting the independent variable  $P_i$  in Equation (2) 1000 times, and the fit to the actual data falls outside that envelope (Supplementary Fig. 7). Thus, we conclude our result is robust with p<0.001.

We note that recent observations suggest variation of As content among genotypes, with *S. natans VIII* having higher As content than *S. natans I* and *S. fluitans III*<sup>20,52</sup>. Because our methods did not distinguish *S. natans VIII*, it would have been grouped together with *S. fluitans III* due to their morphological similarity. Our data do not indicate large variations in As content among the species we resolved (Supplementary Fig. 1, Supplementary Table 1), so this analysis was based on the As content of the combined species.

Cipolloni, O.-A. *et al.* Metals and metalloids concentrations in three genotypes of pelagic *Sargassum* from the Atlantic Ocean Basin-scale. *Marine Pollution Bulletin* **178**, 113564 (2022). https://doi.org/10.1016/j.marpolbul.2022.113564

Gobert, T. *et al.* Trace metal content from holopelagic *Sargassum* spp. sampled in the tropical North Atlantic Ocean: Emphasis on spatial variation of arsenic and phosphorus. *Chemosphere* **308**, 136186 (2022).

https://doi.org:https://doi.org/10.1016/j.chemosphere.2022.136186